Geophysical Research Letters

RESEARCH LETTER
10.1029/2023GL104992

Introducing Flashiness-Intensity-Duration-Frequency (F-IDF): A New Metric to Quantify Flash Flood Intensity

Zhi Li[1,2], Shang Gao[3], Mengye Chen[2], Jiaqi Zhang[2], Jonathan J. Gourley[4], Yixin Wen[5], Tiantian Yang[2], and Yang Hong[2]

[1]Department of Earth System Science, Stanford University, Stanford, CA, USA, [2]School of Civil Engineering and Environmental Science, University of Oklahoma, Norman, OK, USA, [3]School of Natural Resources and the Environment, Tucson, AZ, USA, [4]National Severe Storms Laboratory, NOAA, Norman, OK, USA, [5]Department of Geography, University of Florida, Gainesville, FL, USA

Key Points:

- We introduce the Flashiness-Intensity-Duration-Frequency curve to quantify flash flood intensity
- The CONUS-wide Flashiness-Intensity-Duration-Frequency values are provided at 3,722 stream gage locations
- The relations between 59 basin attributes and flashiness values are explored

Supporting Information:

Supporting Information may be found in the online version of this article.

Correspondence to:

Y. Hong,
yanghong@ou.edu

Citation:

Li, Z., Gao, S., Chen, M., Zhang, J., Gourley, J. J., Wen, Y., et al. (2023). Introducing Flashiness-Intensity-Duration-Frequency (F-IDF): A new metric to quantify flash flood intensity. *Geophysical Research Letters*, *50*, e2023GL104992. https://doi.org/10.1029/2023GL104992

Received 13 JUN 2023
Accepted 1 NOV 2023

Author Contributions:

Conceptualization: Zhi Li, Yang Hong
Data curation: Zhi Li
Formal analysis: Zhi Li
Investigation: Zhi Li, Shang Gao
Methodology: Zhi Li, Shang Gao, Jiaqi Zhang, Jonathan J. Gourley
Project Administration: Yang Hong
Software: Zhi Li
Supervision: Yang Hong
Validation: Zhi Li, Mengye Chen
Visualization: Zhi Li, Yixin Wen
Writing – original draft: Zhi Li

Abstract

Flash flooding is a damaging weather event, yet it remains challenging to quantify its severity. We propose a development—the Flashiness-Intensity-Duration-Frequency (F-IDF) curve—to quantify flash flood intensity based on the frequency and duration of the event. As a proof-of-concept, we mapped Contiguous US (CONUS)-wide F-IDF values at 3,722 stream gage locations and explored their relations with basin attributes. It is found that (a) The return periods of flash flood events are highly associated with the return peroids of rainfall events; (b) Climatological precipitation amounts exhibit the most positive correlation with flashiness while a basin's drainage area is the most negatively correlated; (c) Correlation of flashiness with basin attributes decreases with increasing F-IDF return periods and shorter event durations. Both aspects are attributable to the rainfall signal overwhelming the underlying basin attributes as the intensities become more extreme. This new metric has implications for hydrology and emergency responders.

Plain Language Summary

Flash floods are among the most devasting natural hazard types that can cause severe property damage and loss of life. However, it's challenging to measure and quantify the severity. This study proposes a new way of quantifying flash flood intensity using a newly developed Flashiness-Intensity-Duration-Frequency (F-IDF) curve. It links flash flood severity with how often they happen and how long they last. We mapped F-IDF values across the United States and found that certain areas are more prone to flash floods than others. The amount of rain and the size of the basin area are the most important factors in determining how severe a flash flood is. This new quantification tool can help experts better identify and respond to flash flood risks.

1. Introduction

Flash floods are a type of flood that occurs within minutes to several hours of heavy rainfall or other causes (Doswell III, 2015; Gourley et al., 2013; Hong et al., 2013). In recent years, fatalities and damages caused by flash flooding have been increasing worldwide, making it one of the most destructive weather types (Ashley & Ashley, 2008).

To identify flash flood risks, researchers have sought various approaches. One of the most common practices for flash flood warnings over the US and the world is the Flash Flood Guidance (FFG) (Georgakakos et al., 2022). It has been adopted as the operational early warning system for flash flooding by the US National Weather Service since the 1970s (Georgakakos, 1986). FFG is defined as an estimate of total rainfall that causes bankful flow. As it suggests, this method does not take into account the full continuum of land surface responses to extreme rainfall and river routing processes. Beyond FFG, there are other attempts to quantify flash flood risks. We generalize them into event-dependent and event-independent approaches. An event-dependent approach directly calculates flash flood risks based on archived flash flood events (Alipour et al., 2020) or a flashiness index (Gannon et al., 2022; Li et al., 2022; Saharia et al., 2017, 2021; Smith & Smith, 2015). The term flashiness index was introduced to measure how quickly and how high streamflow rises in an event (Baker et al., 2004). Among variants of the flashiness index, the Richards-Baker Flashiness Index (RBI) is one of the earliest indices, denoted by the time derivative of daily streamflow (Baker et al., 2004). Gannon et al. (2022) evaluated the RBI at daily time scales and found little or no correspondence between basin responses and watershed areas. This result differs from Saharia et al. (2017) who revealed a significant relationship of increasing flashiness with smaller

Writing – review & editing: Zhi Li, Shang Gao, Mengye Chen, Jiaqi Zhang, Jonathan J. Gourley, Yixin Wen, Tiantian Yang, Yang Hong

watersheds, with the discrepancy being attributed to the latter study's use of sub-hourly stream gage data instead of daily. Since it is event-dependent, this approach presumably delivers accurate and precise results. Alternatively, an event-independent approach seeks a statistical model that relates climate variables and basin physiography to flash flood risks (Lin et al., 2020; Ma et al., 2019). In doing so, this approach bypasses the requirement for observations, which is particularly useful in ungauged basins or rural regions. Its validity, however, requires particular attention.

Given the dense stream gage network in the US, we propose a new method using the flashiness index applied to specific events. Although the definition of flashiness is diverse, this study adopts the approach of estimating the slope of the rising limb of the hydrograph. The flashiness index used in previous studies is only a static quantity that is irrespective of event frequency and duration (Li et al., 2022; Saharia et al., 2017, 2021; Smith & Smith, 2015). Weather forecasters, emergency responders, and the public are particularly concerned about the risk of a flash flood event, which can be quantified by frequency. Additionally, we particularly value the representativeness of this index with respect to simplicity and reproducibility. In light of these concerns, we adopt the idea from the Rainfall Intensity-Duration-Frequency (R-IDF) curve that encapsulates three-dimensional information of a rainfall event (Perica et al., 2013), and apply it to quantify a flash flood event. Hence, we introduce the Flashiness-Intensity-Duration-Frequency (F-IDF) curve for the first time. Similar to the R-IDF curve, the F-IDF curve describes the intensity (based on flashiness values), duration, and frequency of flash flood events. We envision that such a measure has practical implications in flash flood forecasting and risk management. The aim of this article is threefold: (a) introducing the methods of calculating a F-IDF curve; (b) mapping F-IDF values for all US stream gages; and (c) investigating geographical and hydrometeorological factors associated with F-IDF values. The newly introduced F-IDF curve can be applied to observed or simulated hydrographs, meaning that it can be integrated into any flood forecast system.

2. Materials and Methods

2.1. Flashiness-Intensity-Duration-Frequency

The F-IDF curves in this study are computed as follows: (a) Select flood events by which streamflow exceeds a 2-year threshold; (b) Find the maximum rising (positive) slope S of a hydrograph using a recursive moving time window (i.e., $D = 1$, 2, 3, 4, 5, and 6 hr); (c) Concatenate flashiness values and extract the seasonal maxima for each duration D; (d) Fit the seasonal maxima into a general extreme value distribution (GEV) and logPearson Type III distribution (LP3); (e) Find an optimal fit based on the Bayesian Information Criterion; and (f) Return flashiness values for different frequencies (i.e., 1-in-2-year, 1-in-5-year, 1-in-10-year, 1-in-25-year, 1-in-50-year, and 1-in-100-year). The resulting flashiness value F is a measure of rapidness and magnitude changes over the time window and is represented in Equation 1. An illustrative example is given in Figure 1a.

$$F = \frac{\max\{O_t - O_{t-1}, O_t - O_{t-2}, \ldots O_t - O_{t-d}\}}{\mathrm{FAC} \times d}, \tag{1}$$

where O_t is the observed streamflow time series at time t, d is the duration, FAC is the drainage area (km^2). The unit of F is dependent on the observation but is generally expressed in units of [L/T^2]. We standardize the unit of flashiness value to be measured in mm/h^2. In this study, we use the USGS stream gage record at a 15-min time interval, so a conversion factor 0.4078 is applied to convert ft^3/s/km^2/15-min to mm/h^2.

Repeating the process of calculating flashiness values at different durations and different frequencies, we can depict the F-IDF curve as shown in Figure 1b for one streamgage site. The shape of the F-IDF is similar to the R-IDF, where intensity decreases with longer duration but increases with event rarity.

There are several noteworthy points in calculating F-IDF values. First, because flash floods typically occur within 6 hr of the causative rainfall, we did not consider events with durations greater than 6 hr. Second, the rationale for selecting seasonal maxima rather than annual maxima is two-fold: (a) Increase sample sizes; (b) Capture multi-modal rainfall peaks across different seasons. Third, we select two extreme value distributions in this study: (a) LP3 distribution and (b) GEV distribution. The LP3 distribution is a common approach in hydrologic frequency analysis, recommended by the US Water Resources Council (England et al., 2017; Singh, 1998). The GEV is an alternative approach that harmonizes the type I, type II, and type III extreme value distributions into a single family to allow a continuous range of possible shapes. Wallis and Wood (1985) compared LP3 and GEV

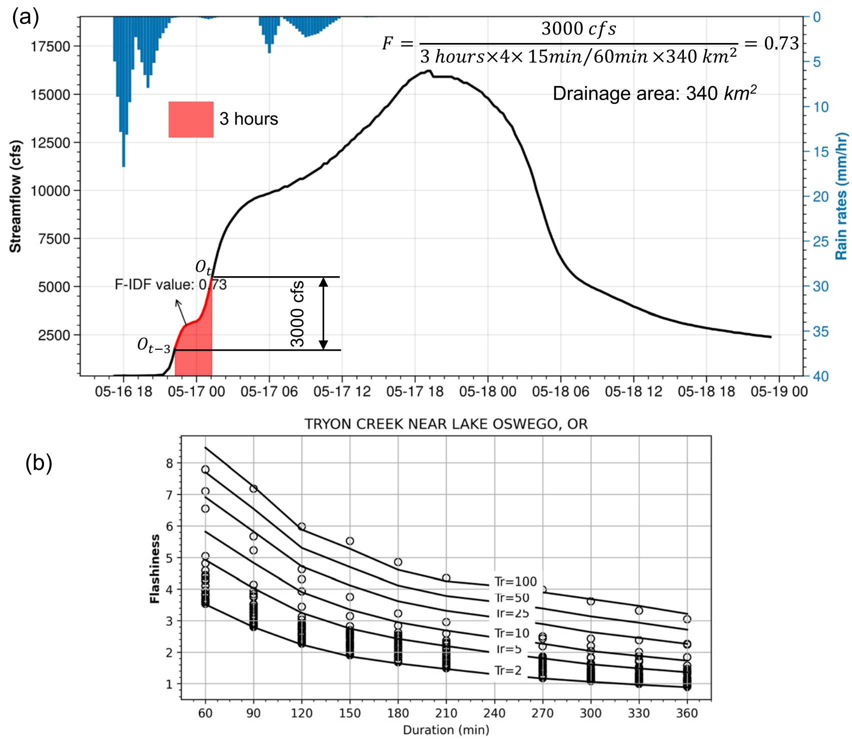

Figure 1. (a) An illustrative example of calculating Flashiness-Intensity-Duration-Frequency values. The figure is produced with the Python Matplotlib library; (b) the empirical F-IDF plot and points are real events that surpass 2-year flashiness values.

distribution and found the goodness-of-fit for the two methods varied across different sites, indicating the need to diversify GEV distribution methods. Third, given the short gage record length (average 22.3 years over the entire set of records), we only extrapolate return periods to 100 years; otherwise, there are large uncertainties associated with the fitted GEV model (details refer to Section 3.1).

3. Data

3.1. CONUS-Wide Streamflow

We intended to collect 15-min streamflow time series data for all stream gages over the CONUS from 1950 to 2020. However, not all gauge sites have continuous data, especially at a sub-hourly frequency. A map of stream gage data length distribution is shown in Figure S1 of the Supporting Information S1. We filter out gages that have available data of less than 20 years to ensure enough data samples for fitting the extreme value distributions. There are 3,722 gages left after filtering. Next, we harmonize an equal time interval of 15 min for all stream gages by using linear interpolation because some gages have an interval of 30 min. The linear interpolation method is often used to fill in gaps in streamflow data (Petrone et al., 2010).

3.2. Catchment Attributes

To analyze the flashiness values with basin characteristics, we use the basin attributes from the HydroATLAS data set (Linke et al., 2019). These attributes include eight sections: Hydrology (i.e., annual runoff, precipitation, natural discharge, inundation extent, groundwater table, river area, and river volume), Physiography (i.e., channel slope, catchment slope, elevation, and drainage area), Climate (i.e., annual precipitation, potential evaporation, actual evaporation, climate moisture index, aridity index, air temperature, snow cover), Soils & Geology (i.e., soil water content—average water in soils, clay fraction, silt fraction, sand fraction, karst fraction, soil erosion), Human (i.e., road density, urban density, population), Land Cover (i.e., area extent of trees, shrubs,

10.1029/2023GL104992

herbaceous, cultivated land, water bodies, snow, and artificial lands—constructed or interfered by human rather than formed naturally), Natural Vegetation (i.e., evergreen, deciduous, savanna, grassland, tundra, desert), and Wetland (i.e., lake reservoir, river, and peatland). There are 59 basin attributes in total used in this study. We spatially join these attributes to the catchments of all stream gages and use the values representing the total watershed upstream of the gage. A detailed description of these attributes is provided in Linke et al. (2019).

4. Results

4.1. Mapping CONUS-Wide F-IDF Values

After iterating through steps 1–5 in Section 2.1 for each stream gage, we can map the CONUS-wide F-IDF values. Figure 2 shows the 1-hr flashiness values at six return periods (2-year, 5-year, 10-year, 25-year, 50-year, and 100-year) as an example. Maps for other durations (i.e., 2-hr, 3-hr, 4-hr, 5-hr, and 6-hr) can be found in Figures S2–S6 of the Supporting Information S1. **A general observation for these maps as indicated in Figure 1b is that F-IDF values decrease with frequency and duration, in a similar manner as with R-IDF values**. We can identify flashy regions in the CONUS by clustering stream gages that have flashiness values larger than 1 (shown in Figure 2). Those five regions are (a) the West Coast, (b) the Missouri Valley, (c) the Appalachians, (d) Flash Flood Alley (Central Texas), and (e) Southwest. The results agree well with Saharia et al. (2017) and Li et al. (2022), despite slight differences in defining the flashiness variable. We also compared our results with real flash flood events from 1970 to 2020 in a newly developed US flood database (Figure S7 in Supporting Information S1; Li et al., 2021). These flash flood events were verified by the US National Weather Service. Our identified regions also emerge, except for the Pacific Northwest region, which has a low incidence of flash flood reports. A similar finding is reached by Smith and Smith (2015), who reported the differences are in nature due to different measures.

The main drivers for flash floods are region-dependent. On the West Coast, the main atmospheric agent for flash flooding is atmospheric rivers, which transport considerable moisture from the tropics to mid-latitudes. Even though atmospheric rivers produce long-duration winter rainfall and snowfall, the steeply sloped terrain and compact watersheds can generate fast-rising runoff (Saharia et al., 2017; Smith & Smith, 2015). Further inland, the contributions of warm-season thunderstorms to flash flood occurrences start to dominate, especially for the Missouri Valley (Region 2) and Flash Flood Alley region (Region 4). Flash floods are frequently instigated by training thunderstorms (a series of thunderstorms passing through the region with only short breaks in between). Flash Flood Alley also bears frequent tropical cyclones and hurricanes off the Gulf Coast. The Appalachians (Region 3) are another known hot spot for flash flooding, extending from Georgia up to Maine. Besides the hilly terrain, extratropical cyclones are the synoptic weather types that frequently hit this region and result in a sequence of flood events (Li et al., 2021). The Southwest (Region 5) is renowned for its hot and dry environment that initiates convective thunderstorms during the North American monsoon season (Smith et al., 2019). Besides the atmospheric forcings, land surface conditions such as impervious area ratio, antecedent soil moisture, groundwater level, catchment drainage density, etc., jointly determine flash flood hazard.

4.2. Causative Analysis Between Extreme Rainfall Events and Flashiness

The primary causative factor of flash floods is extreme rainfall. We associate the F-IDF with the R-IDF on an event basis using flash flood event reports coordinated by the National Weather Service from 1 June 2018 to 31 May 2019 (Li et al., 2021). We retrieve the event rainfall data from the Multi-Radar Multi-Sensor (MRMS) hourly rainfall records for the stream gauge accumulating basin. Subsequently, for respective rainfall event durations (1-hr, 2-hr, 3-hr, 6-hr, 12-hr, and 24-hr), we compare the event rainfall with R-IDF from the NOAA Atlas 14 product to ascertain the return periods. We replicate this process for flashiness to derive flashiness return periods.

Figure 3 illustrates the number of events characterized by different return periods of R-IDF and F-IDF. First, 100-year rainfall events trigger the majority of flash flood events across various rainfall and flash flood event durations, with the only exception being the 1-hr rainfall event where 10-year rainfall induces the maximum number of flash flood events. Second, an upward trend of rainfall return periods correlating with an increase in flash flood events is observed. While lower return periods of flashiness are instigated by all rainfall return periods, rare return periods of flashiness are exclusively triggered by more extreme rainfall. Lastly, a decline in the number of events corresponds with the extension of flash flood event durations, attributable to a greater sample size for shorter-duration flash flood events.

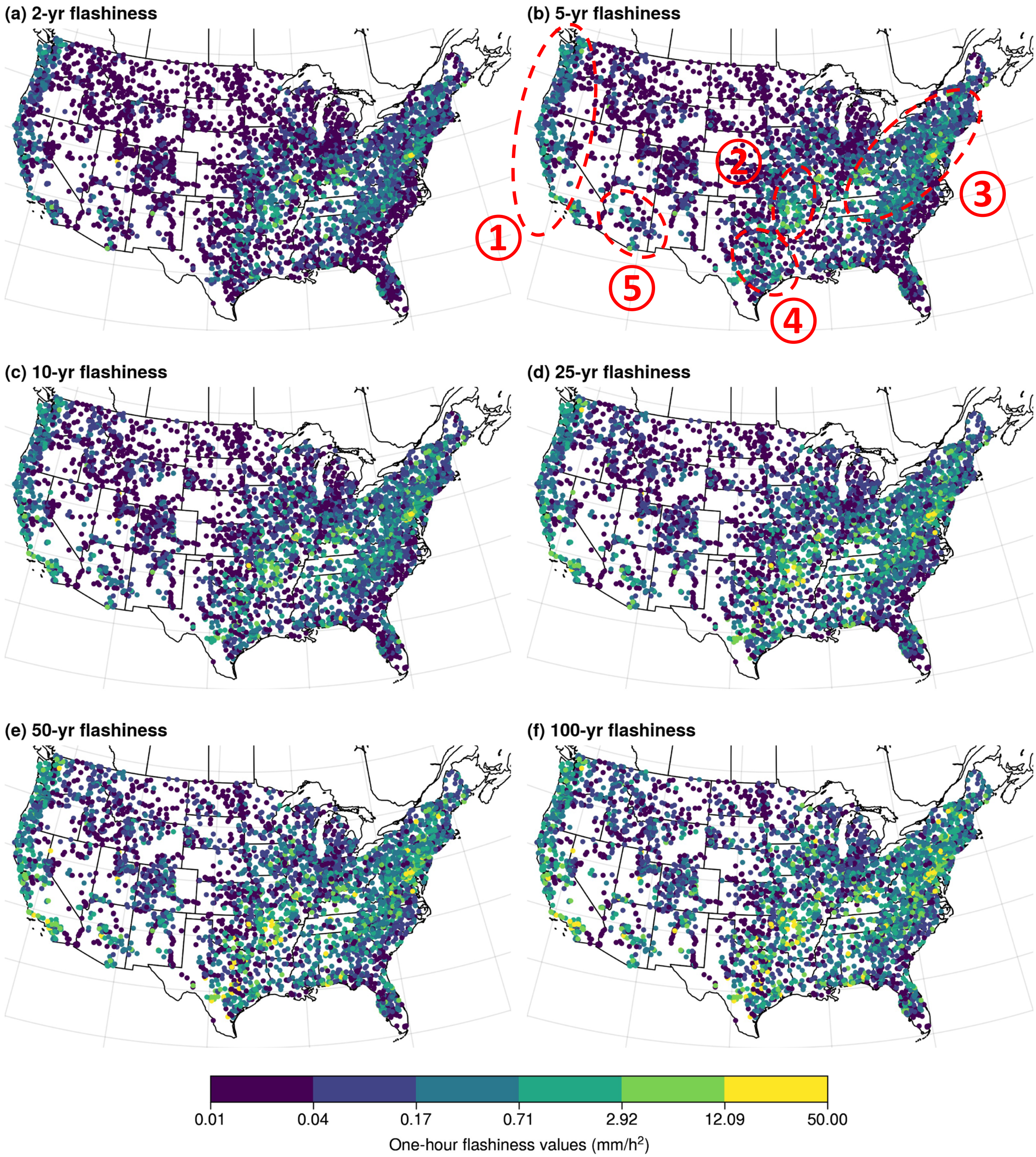

Figure 2. Maps of F-IDF values at 1-hr duration. Highlighted (numbers from 1 to 5) regions are clustered flashy regions in the CONUS. 1: West Coast; 2: Missouri Valley; 3: the Appalachians; 4: Flash Flood Alley; and 5: Southwest.

4.3. Geographical Factors Related to Flashiness Values

We present a comprehensive view of factors determining flashiness values by utilizing 59 basin attributes and analyzing their correlation with flashiness. Figure 4a depicts the Spearman Correlation Coefficient (CC) between

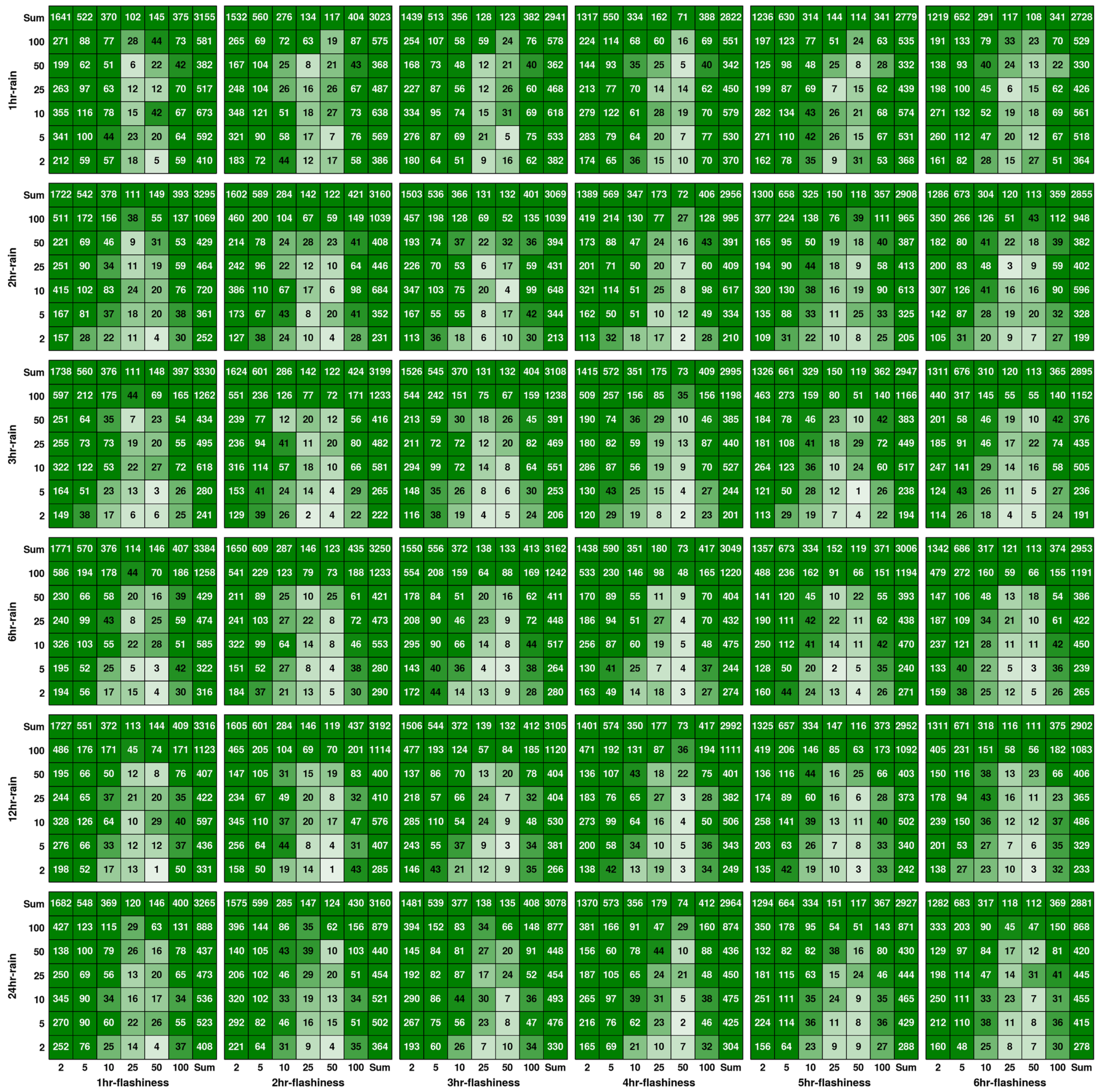

Figure 3. Heatmaps of numbers of events associated with rainfall return periods (i.e., 2, 5, 10, 25, 50, and 100) and flashiness return periods (i.e., 2, 5, 10, 25, 50, and 100) at different durations. The "Sum" is the summation of event numbers for corresponding columns or rows.

flashiness values and 59 basin attributes across 3,722 gage sites. For each site, we have CCs for six event durations and six return periods, but only the minimum, median, and maximum values are shown in the table. Overall, **climate** exerts the most positive correlation with flashiness values, with annual precipitation ranked 1st place (Median CC = 0.49), followed by actual evaporation and moisture and aridity index (CC = 0.45), and air temperature (CC = 0.32). It's worth noting that the aridity index is positively related to the amount of moisture in the land. In other words, the lower the aridity index, the drier the land is. **Hydrologic variables** are mostly negatively correlated with flashiness in decreasing order: natural discharge (CC = −0.32), degree of regulation (CC = −0.36), river volume (CC = −0.46), and river area (CC = −0.50). The exception is land surface runoff which has a positive CC of 0.43. **Physiographic variables** exhibit a negative correlation with flashiness, with

10.1029/2023GL104992

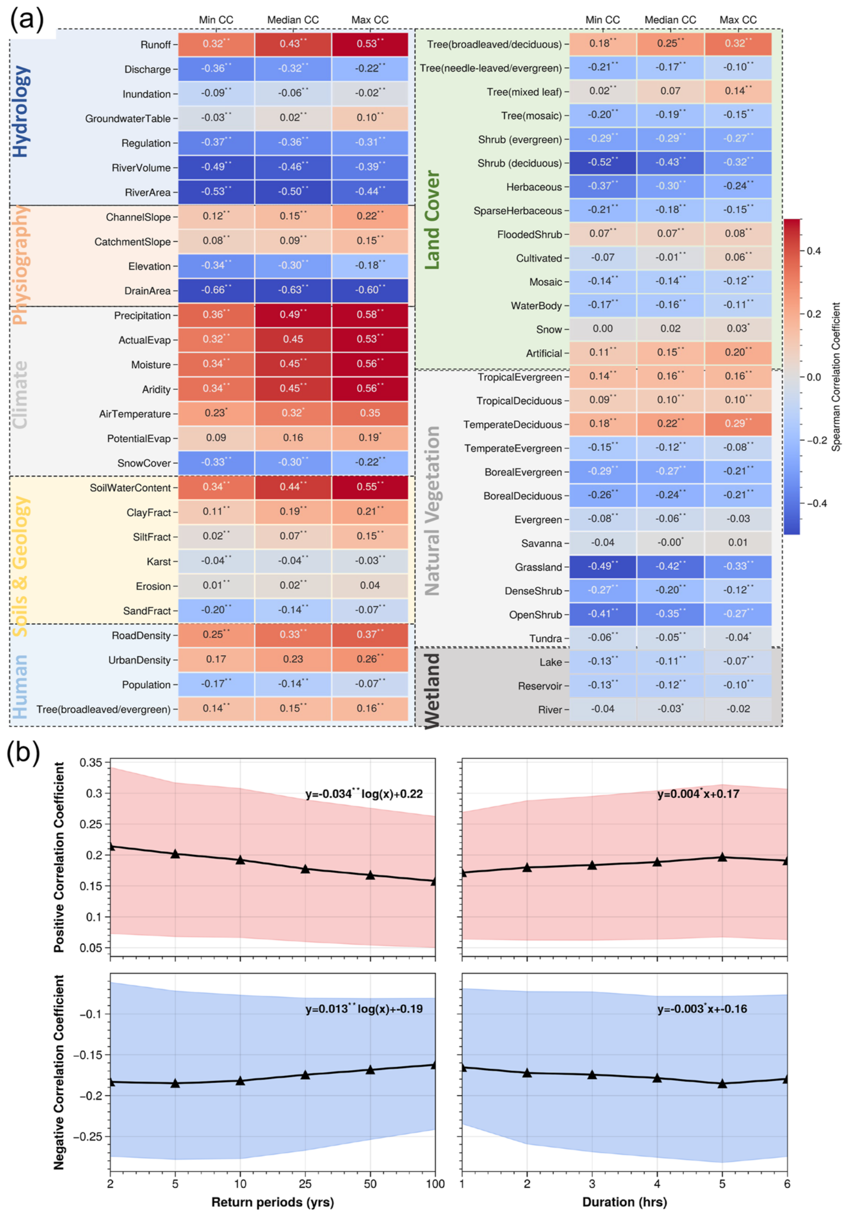

Figure 4. (a) A table of Spearman Correlation Coefficients between flashiness and filtered basin attributes. A single asterisk (*) indicates a 95% confidence level, and two asterisks (**) indicate a 99% confidence level to reject a null hypothesis (zero correlation). (b) Plots of positive and negative correlation coefficients (by aggregating respective variables) with respect to return periods and duration. The black dotted line shows the mean correlation coefficient while the band shows the interquartile range from Q25 to Q75. The significance of the slope is tested against a zero slope using the general linear F-statistic with the fitted regression model.

elevation (CC = −0.30) and drainage area (CC = −0.63) being the most significant factors. The **soils & geology** group has a relatively weak association with flashiness. Soil water content has the greatest CC of 0.44 within this class, followed by clay fraction (CC = 0.19), silt fraction (CC = 0.07), and sand fraction (CC = −0.14). The **human** group shows positive correlations with road density (CC = 0.33) and urban density (CC = 0.23) being the most significant ones. The notable features in the **land cover** group are deciduous trees (CC = 0.25), artificial surface (CC = 0.15), herbaceous (CC = −0.30), and deciduous shrubs (CC = −0.43). Similar to land cover, the **natural vegetation** group shows the temperate deciduous region has a positive correlation (CC = 0.22) with flashiness, while grassland (CC = −0.42), open shrub (CC = −0.35), boreal evergreen (CC = −0.27), and boreal deciduous (CC = −0.24) have negative correlations. The **wetland** group does not exhibit a significant positive correlation.

The controlling factors above can be summarized as follows. First, small river reaches tend to have higher flashiness values, as the negative correlations between river area, volume, and natural discharge testify to this point. Second, flood defense infrastructures impede flash flood generation, as indicated by the negative impact of the degree of regulation. Third, flashiness is highly related to wetness or annual precipitation. Fourth, flash floods are typically not snowmelt-driven processes as seen with the weakly negative correlations to snow cover. Fifth, regarding soil types, the degrees of soil types contributing to flashiness are ranked as: clay > silt > sand, which is a reversed order of permeability. Sixth, wet soils, urban density, and road density help generate flash floods by impeding soil infiltration. Lastly, dense vegetation and land cover (e.g., shrub and grassland) increase surface roughness and thus negatively correlate with flashiness.

We divide the 59 factors into positive correlation and negative correlation and plot their respective changes with regard to return periods and durations in Figure 4b. The significance of each slope is tested against a zero slope with the general linear F-statistics (Gordon, 2012). As the occurrence of flash flood events becomes less frequent (i.e., larger return period), the absolute correlation coefficient decreases. When reaching higher levels of intensity (i.e., 100-year event), the event flashiness is less influenced by basin attributes as the causative rainfall emerges as the primary driver. The correlation coefficients increase with the duration of the event (see Figures 4b and 4d). Likewise, correlation increases with longer-duration events, as shown in the F-IDF curve in Figure 1b, and becomes more influenced by basin attributes.

5. Discussion

5.1. The Representativeness of Flashiness Index

In this study, we chose the maximum sub-hourly time derivative of streamflow over a time window as the basis for building the F-IDF curves. First, using data collected at a time scale appropriate for the application requires consideration. For investigations of flash flooding, a sub-hourly time step is ideal. Acknowledging many other variants of flashiness indices (Gannon et al., 2022; Kim & Choi, 2011; Saharia et al., 2017, 2021; Smith & Smith, 2015), this approach has several benefits. First, it is fairly simple, reproducible, and easy to comprehend. Second, it represents both the flood magnitude and flood rising limb, which is the nature of the term "flashiness" introduced by Baker et al. (2004).

This study only considers flash flood events with durations less than 6 hr which is a common definition for flash flooding (Clark et al., 2014). But for large basins (where the time of concentration is long) or long-duration storms, this duration of F-IDF can be further extended to 12 and 24 hr by tuning the time window parameter in Equation 1.

5.2. Correlation With Basin Attributes

We calculated the Spearman Correlation Coefficient of flashiness index against 59 basin attributes acquired from the HydroATLAS. As noted, the CC values are generally low (CC < 0.7) for those factors. That is mainly because flash flooding, by nature, is a dynamic weather-driven phenomenon that is challenging to predict by static features (such as basin slope and annual precipitation). Similarly, Smith and Smith (2015) found that most of the CCs of a number of flash flood peaks with basin attributes are lower than 0.6. Second, the CC values are calculated with a uni-variate analysis, but we expect a higher value if we choose a multi-variate analysis, such as regression models and/or machine learning models. Since the main focus of this study is to provide a proof-of-concept of the flashiness index, we will explore the predictability of a statistical model in a future work.

5.3. Implications for Hydrologic Science and Flash Flood Response

Our proposed new metric—F-IDF curve, has implications not only for hydrologic science but also for flash flood preparedness and responses. For the first time, this study quantifies the frequency of flash floods based on the flashiness variable computed from observed streamflow data, which provides a metric of the rapidity and severity of flooding. The same variable and associated analysis can be applied to streamflow simulations from hydrologic models. Then, the forecast flashiness and its associated frequency for a given duration can be provided ahead of time. Weather forecasters can then use such metrics to guide the issuance of flash flood warnings. Additionally, it is worth noting that the implementation of F-IDF curves is model-agnostic, meaning that it can be integrated into any flood forecast system. Second, for hydrologic modelers, the F-IDF curve provides a means of identifying flash flood events. Prior to this study, the identification of a flash flood event was vague and subjective. A common definition—a flood that occurs within 6 hr of a rainfall event—was too obscure for modelers to identify the start and end date of an event. However, with the help of the F-IDF curve, one can easily establish a quantitative threshold to determine a flash flood event. For instance, in a flood study, a 2-year streamflow return period has often been used as a threshold to identify a flood event, given that this threshold approximately corresponds to an overbank flow rate (Dalrymple, 1960). Similarly, we can use a 2-year flashiness value at a particular duration to sift through flash flood events. Third, for city planners and decision-makers, the existing F-IDF values can inform them of the risk of flash floods in the local area (by providing the hazard component in the risk assessment framework). There are undoubtedly other applications beyond those mentioned here. In summary, this newly introduced metric has implications not only for the scientific community but also for its potential role in the science-informed, policy-making process.

6. Conclusions

This article introduces the F-IDF curve to quantify the intensity, duration, and frequency of flash floods adopting a similar concept of the R-IDF curve. The F-IDF curves are quantified for 3,722 US stream gages. We examined the causative relation between R-IDF and F-IDF using 1-year flash flood events over the US. Additionally, the correlation of flashiness with regard to 59 basin attributes is also explored and discussed. The conclusions are drawn as follows:

1. F-IDF curves are capable of revealing the spatial variability of flashy basins across the US and the following places are identified as flash-flood-prone regions: the West Coast, Missouri Valley, Appalachians, Flash Flood Alley in Texas, and the Southwest.
2. The flash flood events in the US are predominately triggered by extreme rainfall. An increase in rainfall return periods corresponds to higher return periods of flash flood events.
3. Among the explored basin attributes, mean annual precipitation is the most positively correlated with flashiness while the basin's drainage area is the most negatively correlated variable.
4. The correlations weaken with increasing return periods and shorter event durations. This is attributable to the extremity of the rainfall overwhelming the influence from underlying basin attributes.

Similar to flood studies, predicting flashiness values in ungauged basins is a grand challenge that warrants scientific exploration. We plan to integrate F-IDF curves into flash flood forecast models over the US and beyond in a future work.

Conflict of Interest

The authors declare no conflicts of interest relevant to this study.

Data Availability Statement

The F-IDF values with joined basin attributes at US stream gages are available at Li (2023) with a Creative Commons Attribution 4.0 International license. The basin attributes are retrieved from Linke et al. (2019). The USGS 15-min streamflow time series is downloaded using the software provided by Hodson et al. (2023).

Acknowledgments
This work is supported by University of Oklahoma Hydrology and Water Security Program.

References

Alipour, A., Ahmadalipour, A., Abbaszadeh, P., & Moradkhani, H. (2020). Leveraging machine learning for predicting flash flood damage in the Southeast US. *Environmental Research Letters*, *15*(2), 024011. https://doi.org/10.1088/1748-9326/ab6edd

Ashley, S. T., & Ashley, W. S. (2008). Flood fatalities in the United States. *Journal of Applied Meteorology and Climatology*, *47*(3), 805–818. https://doi.org/10.1175/2007jamc1611.1

Baker, D. B., Richards, R. P., Loftus, T. T., & Kramer, J. W. (2004). A new flashiness index: Characteristics and applications to midwestern rivers and streams. *Journal of the American Water Resources Association*, *40*(2), 503–522. https://doi.org/10.1111/j.1752-1688.2004.tb01046.x

Clark, R. A., Gourley, J. J., Flamig, Z. L., Hong, Y., & Clark, E. (2014). CONUS-wide evaluation of national weather service flash flood guidance products. *Weather and Forecasting*, *29*(2), 377–392. https://doi.org/10.1175/WAF-D-12-00124.1

Dalrymple, T. (1960). *Flood-frequency analyses, manual of hydrology: Part 3 (No. 1543-A)*. USGPO.

Doswell, C. A., III. (2015). Hydrology, floods and droughts: Flooding. In *Encyclopedia of atmospheric sciences* (2nd ed., pp. 201–208). https://doi.org/10.1016/B978-0-12-382225-3.00151-1

England, J. F., Jr., Cohn, T. A., Faber, B. A., Stedinger, J. R., Thomas, W. O., Jr., Veilleux, A. G., et al. (2017). Guidelines for determining flood flow frequency—Bulletin 17C: U.S. geological survey techniques and methods book 4, chapter B5. (p. 148). https://doi.org/10.3133/tm4B5.March2018

Gannon, J., Kelleher, C., & Zimmer, M. (2022). Controls on watershed flashiness across the continental US. *Journal of Hydrology*, *609*, 127713. https://doi.org/10.1016/j.jhydrol.2022.127713

Georgakakos, K. P. (1986). On the design of national real-time warning systems with capability for site-specific, flash-flood forecasts. *Bulletin of the American Meteorological Society*, *67*(10), 1233–1239. https://doi.org/10.1175/1520-0477(1986)067<1233:otdonr>2.0.co;2

Georgakakos, K. P., Modrick, T. M., Shamir, E., Campbell, R., Cheng, Z., Jubach, R., et al. (2022). Flash flood guidance system implementation worldwide: A successful multidecadal research-to-operation effort. *Bulletin of the American Meteorological Society*, *103*(1), E1–E22. https://doi.org/10.1175/BAMS-D-20-0032.1

Gordon, R. A. (2012). *Applied statistics for the social and health sciences*. Routledge.

Gourley, J. J., Hong, Y., Flamig, Z. L., Arthur, A., Clark, R., Calianno, M., et al. (2013). A unified flash flood database across the United States. *Bulletin of the American Meteorological Society*, *94*(6), 799–805. https://doi.org/10.1175/BAMS-D-12-00198.1

Hodson, T. O., Hariharan, J. A., Black, S., & Horsburgh, J. S. (2023). *Dataretrieval (Python): a Python package for discovering and retrieving water data available from U.S. federal hydrologic web services*. U.S. Geological Survey Software Release. https://doi.org/10.5066/P94I5TX3

Hong, Y., Adhikari, P., & Gourley, J. J. (2013). Flash flood. In P. T. Bobrowsky (Ed.), *Encyclopedia of natural hazards. Encyclopedia of Earth sciences series*. Springer. https://doi.org/10.1007/978-1-4020-4399-4_136

Kim, E., & Choi, H. (2011). Assessment of vulnerability to extreme flash floods in design storms. *International Journal of Environmental Research and Public Health*, *8*(7), 2907–2922. https://doi.org/10.3390/ijerph8072907

Li, Z. (2023). F-IDF values at USGS stream gage sites (v1.0) [Dataset]. Zenodo. https://doi.org/10.5281/zenodo.7806694

Li, Z., Chen, M., Gao, S., Gourley, J. J., Yang, T., Shen, X., et al. (2021). A multi-source 120-year US flood database with a unified common format and public access. *Earth System Science Data*, *13*(8), 3755–3766. https://doi.org/10.5194/essd-13-3755-2021

Li, Z., Gao, S., Chen, M., Gourley, J., Liu, C., Prein, A. F., & Hong, Y. (2022). The conterminous United States are projected to become more prone to flash floods in a high-end emissions scenario. *Communications Earth and Environment*, *3*(1), 86. https://doi.org/10.1038/s43247-022-00409-6

Lin, K., Chen, H., Xu, C., Yan, P., Lan, T., Liu, Z., & Dong, C. (2020). Assessment of flash flood risk based on improved analytic hierarchy process method and integrated maximum likelihood clustering algorithm. *Journal of Hydrology*, *584*, 124696. https://doi.org/10.1016/j.jhydrol.2020.124696

Linke, S., Lehner, B., Ouellet Dallaire, C., Ariwi, J., Grill, G., Anand, M., et al. (2019). Global hydro-environmental sub-basin and river reach characteristics at high spatial resolution. *Scientific Data*, *6*(1), 283. https://doi.org/10.1038/s41597-019-0300-6

Ma, M., Liu, C., Zhao, G., Xie, H., Jia, P., Wang, D., et al. (2019). Flash flood risk analysis based on machine learning techniques in the Yunnan Province, China. *Remote Sensing*, *11*(2), 170. https://doi.org/10.3390/rs11020170

Perica, S., Martin, D., Pavlovic, S., Roy, I., Laurent, M. S., Trypaluk, C. A. R. L., et al. (2013). *NOAA atlas 14 volume 9 version 2, precipitation-frequency atlas of the United States, southeastern states* (p. 18). NOAA, National Weather Service.

Petrone, K. C., Hughes, J. D., Van Niel, T. G., & Silberstein, R. P. (2010). Streamflow decline in southwestern Australia, 1950–2008. *Geophysical Research Letters*, *37*(11), L11401. https://doi.org/10.1029/2010GL043102

Saharia, M., Kirstetter, P.-E., Vergara, H., Gourley, J. J., Emmanuel, I., & Andrieu, H. (2021). On the impact of rainfall spatial variability, geomorphology, and climatology on flash floods. *Water Resources Research*, *57*(9), e2020WR029124. https://doi.org/10.1029/2020WR029124

Saharia, M., Kirstetter, P. E., Vergara, H., Gourley, J. J., Hong, Y., & Giroud, M. (2017). Mapping flash flood severity in the United States. *Journal of Hydrometeorology*, *18*(2), 397–411. https://doi.org/10.1175/jhm-d-16-0082.1

Singh, V. P. (1998). Log-Pearson type III distribution. In *Entropy-based parameter estimation in hydrology. Water science and technology library* (Vol. 30). Springer. https://doi.org/10.1007/978-94-017-1431-0_15

Smith, B. K., & Smith, J. A. (2015). The flashiest watersheds in the contiguous United States. *Journal of Hydrometeorology*, *16*(6), 2365–2381. https://doi.org/10.1175/JHM-D-14-0217.1

Smith, J. A., Baeck, M. L., Yang, L., Signell, J., Morin, E., & Goodrich, D. C. (2019). The paroxysmal precipitation of the desert: Flash floods in the southwestern United States. *Water Resources Research*, *55*(12), 10218–10247. https://doi.org/10.1029/2019WR025480

Wallis, J. R., & Wood, E. F. (1985). Relative accuracy of Log Pearson III procedures. *Journal of Hydraulic Engineering*, *111*(7), 1043–1057. https://doi.org/10.1061/(asce)0733-9429(1985)111:7(1043)